Circuit Modeling of Defected Waveguide Structure

S. J. Chin, M. Z. A. Abd. Aziz and M. R. Ahmad
Centre for Telecommunication Research and Innovation (CeTRI), Faculty of Electronic and Computer Engineering, Universiti Teknikal Malaysia Melaka (UTeM), 76100 Durian Tunggal, Melaka, Malaysia.
shujia2605@gmail.com

***Abstract*—Recently, waveguide has been applied widely in antenna and filter applications. Among these applications, substrate integrated waveguide has been implemented mostly in millimeter wave systems due to its compact and low loss approach. However, the configuration of waveguide itself receives less attention. Thus, the study of defected waveguide structure (DWS) is presented. The copper and DWS waveguide were designed in CST Microwave software. The basic geometry of square was used and then different types of connecting strips were added on in between the strips. Simulated reflection coefficient (S11) and transmission coefficient (S21) results were then modeled by equivalent circuit design. The circuit was constructed in Advanced Design System (ADS). Copper waveguide performed high pass at frequency more than cut off frequency of 2.76GHz. The square DWS with gap separation and square DWS with horizontal connecting strips showed pass band around 4GHz-8GHz. The square DWS with vertical connecting strips and square DWS with both horizontal and vertical connecting strips created band stop around 3GHz-9GHz.**

***Index Terms*—Circuit Modeling; Defected Waveguide Structure; Filter; Ultrawideband.**

I. INTRODUCTION

In communication system, waveguide acts as a medium to transmit and receive signal. It provides high power handling and low loss. However, it is bulky and expensive in cost. It has been used to design for antenna and filter applications [1-4]. In [1], the waveguide antenna with parallel strips that are rotated by 45 degrees at the surface is designed for base station application to achieve polarization rotation. Substrate integrated waveguide (SIW) receives a great attention as it is easy to design to be implemented in planar circuit [2]. Besides that, the waveguide also has been designed with metamaterial to analyze the transmission characteristic [5].

Meanwhile, the defected structure is one of the families of metamaterial since it changes the characteristics of material artificially. It can be defined as some of copper is removed at the surface. Previously, defected structure is designed at the ground plane and the microstrip line is designed as defected ground structure (DGS) and defected microstrip structure (DMS) respectively [6-9]. For example, DGS for [6] is designed on compact printed monopole antenna to enhance bandwidth and reduce size, while DMS for [9] is used to create stop band. There is a lack of information on the design of defected waveguide structure (DWS). Thus, the aim of this paper is to introduce DWS by designing the defected structure at waveguide.

The waveguide is designed to support ultrawideband (UWB) frequency range. The defected structure is designed at the waveguide at fixed length to compare with copper waveguide. The effects of DWS towards waveguide will be investigated through the reflection coefficient (S11) and transmission coefficient (S21).

II. DEFECTED WAVEGUIDE STRUCTURE DESIGN

The rectangular waveguide is designed by using FR4 and copper. The inner wall of waveguide is the copper surface. The dimension of waveguide will determine the cut off frequency f_c , where a and b represent the width and height of the waveguide respectively, as shown in Equation 1 [10]. The dimension of the waveguide should be large enough to support the largest wavelength in UWB frequency range.

$$f_c = \frac{1}{2\pi\sqrt{\mu\varepsilon}}\sqrt{\left(\frac{m\pi}{a}\right)^2 + \left(\frac{n\pi}{b}\right)^2} \quad (1)$$

The copper waveguide is designed, as shown in Figure 1 below. It has the width of 49mm and height of 52mm. Waveguide ports are set at both ends of waveguide.

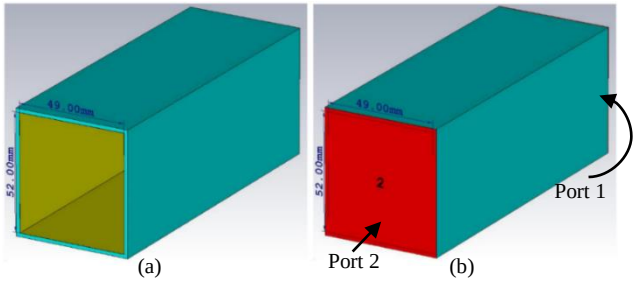

Figure 1: The view of (a) copper waveguide (b) waveguide ports at both ends of waveguide

The defected structure is designed at the inner surface of waveguide by removing some parts of copper as DWS. The DWS is designed in square shape with a gap in between as shown in Design A in Figure 2. There are 15 elements of square used, in which these elements also determine the length of the waveguide. The squares are designed at all the inner walls of waveguide in Figure 3. Both the dimension and the gap in between the squares are optimized. The dimension of 6mm^2 and the gap of 3mm are used since they give the highest S21 and the lowest S11.

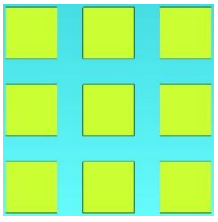

Figure 2: Unit structure of Design A

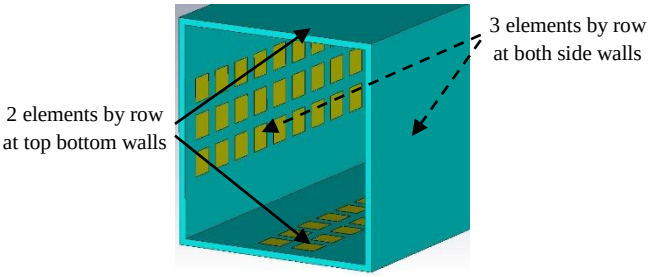

Figure 3: The perspective view of Design A

Design A is further modified to have the strip line connected between squares. The squares are designed to have the horizontal connecting strips (Design B), vertical connecting strips (Design C) or both horizontal and vertical connecting strips (Design D). These three types of connection are showed in Figure 4. Meanwhile, the width of connecting strip is also optimized till the width of 0.5mm is obtained.

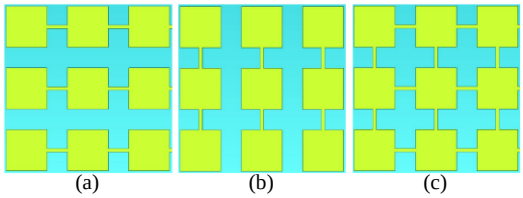

Figure 4: The unit structure of (a) Design B (b) Design C (c) Design D

The transmission and response of all designs will be modelled by using basic equivalent circuit. All the stop band and pass band characteristics will be modelled based on basic filter concept. Filter is designed in a single mode base on maximally-flat low pass filter prototypes. Low pass filter is then scaled in terms of impedance and cut off frequency. The new inductance (L') and the new capacitance (C') of low pass filter can be determined by Equation 2 and Equation 3 [11]. The transformation of low pass filter to other filter is based on filter transformation concept as shown in Figure 5.

$$L' = \frac{RL}{\omega_c} \tag{2}$$

$$C' = \frac{C}{R\omega_c} \tag{3}$$

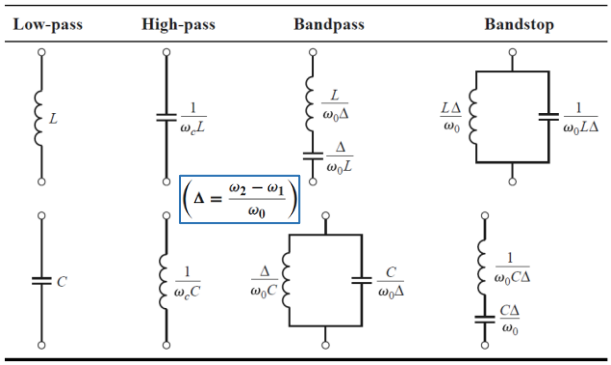

Figure 5: The filter transformation concept [11]

III. RESULTS

The S11 and S21 results were simulated and compared for each design. The simulation was done in separated frequency range of 2GHz-7GHz (low frequency range) and 7GHz-11GHz (high frequency range) to show more accurate result compared to the wideband (2GHz-11GHz). For a significant change in the result, the frequency ranges are showed at 2GHz-6GHz in Figure 6 and 7GHz-11GHz in Figure 7.

The copper waveguide performs high pass at the frequency larger than cut off frequency of 2.76GHz. Design A starts with the lowest S21 of -12.11dB and performs almost a straight line across frequency range. Design B shows low S21 in the frequency range between 2.77GHz and 3.3GHz, where the lowest S21 of -34.52dB occurs at 2.77GHz. Besides that, both the Design A and Design B achieve the highest S21 at 6GHz with value of -3.82dB and -5.23dB respectively. Meanwhile, Design C and Design D have low S21 after 3GHz. Design C achieves the lowest S21 of -56.26dB at 3.21GHz, while Design D achieves the lowest S21 of -37.47dB at 4.1GHz. Both Design C and Design D achieve the highest S21 at lower frequency, which are 2.73GHz and 2.3GHz with S21 of -7.24dB and -9dB.

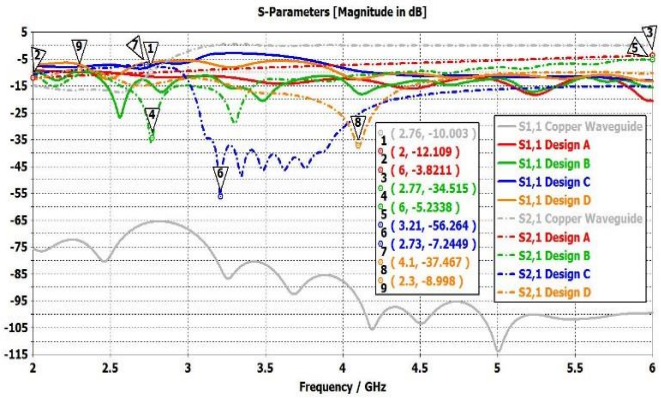

Figure 6: The results of S-parameters of each design at low frequency range (2GHz-6GHz)

At high frequency range of 7GHz-11GHz in Figure 7, the copper waveguide still maintains the highest S21 and the lowest S11 for transmission in Figure 7. Design A and Design B perform high S21 at lower frequency, while low S21 at higher frequency. The highest S21 of Design A is -6.4dB at 7.12GHz and the lowest S21 is -34.64dB at 9.94GHz. Design B achieves the highest S21 of -5.26dB at 7GHz and the lowest S21 of -35.57dB at 10.13GHz. Both Design C and Design D perform the highest S21 at higher frequency of 9.88GHz with S21 -6.83dB and 10.58GHz with S21 -6.57dB respectively. The lowest S21 of Design C occurs at 7GHz with S21 -19.21dB, while Design D occurs at 8.04GHz with S21 -27.54dB.

Overall, copper waveguide performs high pass at frequency more than cut off frequency of 2.76GHz. Design A shows pass band at 2.82GHz-8GHz. Meanwhile, Design B performs pass band at 4.4GHz-8.6GHz. Design C and Design D show stop band around 3GHz-9GHz. These shows that Design A with only square DWS can perform at 2.82GH-8GHz compared to copper waveguide of high pass at 2.76GHz. After adding horizontal connecting strip, Design B shows narrower operation bandwidth of 4.2GHz compared to Design A. Meanwhile, Design B and Design C have opposite responses compared to each other. Design C achieves pass band at 2.1GHz-2.96GHz and 8.5GHz-11GHz. Design A and Design D also show opposite

responses compared to each other. On the contrary, it performs closer responses as Design C with pass band at 2.18GHz-2.42GHz and 9.5GHz-11GHz. This shows that after adding both horizontal and vertical connecting strips, Design D still achieves almost the same response as Design C with vertical connecting strip. Thus, the vertical connecting strips contribute more effects to square DWS compared to horizontal connecting strips.

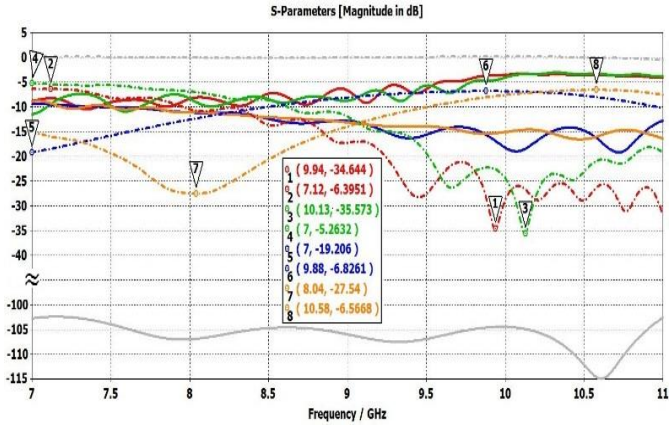

Figure 7: The results of S-parameters of each design at high frequency range (7GHz-11GHz)

Figure 8 shows copper waveguide demonstrates high pass at frequency larger than the cut off frequency at 2.76GHz. In Figure 9 (a), L = 475.4pH is used to perform high pass at low frequency range. At high frequency range, S21 is almost at 0dB, only resistor is acted inside the transmission line that causes negligible loss.

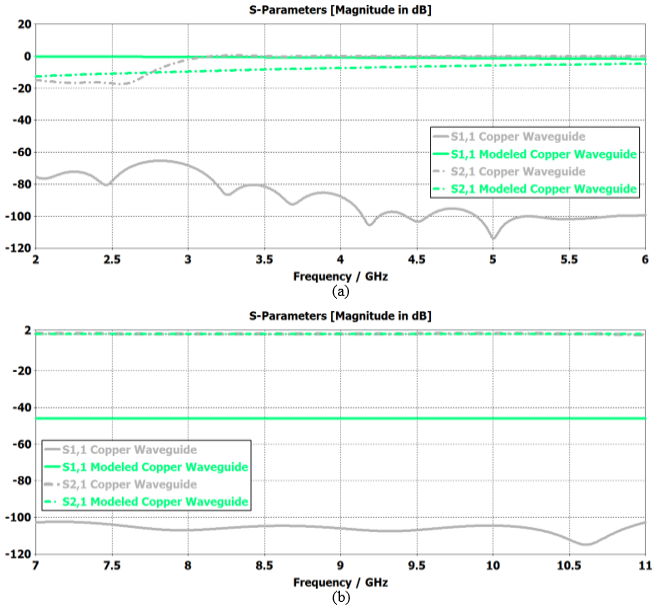

Figure 8: The results of S-parameters from copper waveguide and equivalent circuit design at (a) low frequency range (b) high frequency range

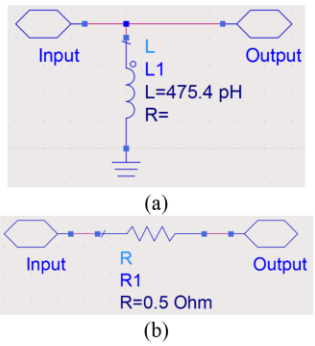

Figure 9: The equivalent circuit design at (a) low frequency range (b) high frequency range

For Design A at low frequency range, $L1$ = 480.19pH is constructed to perform high pass in Figure 11 (a). At high frequency range, the stop band with the lowest S21 of 9.94GHz is created. The value of $L1$ = 499.7pH and $C1$ = 511fF are used to create stop band in Figure 11 (b).

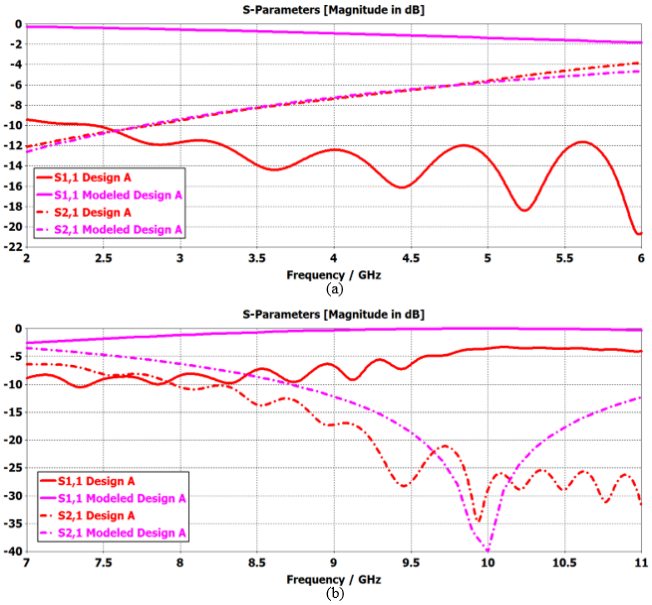

Figure 10: The results of S-parameters from Design A and equivalent circuit design at (a) low frequency range (b) high frequency range

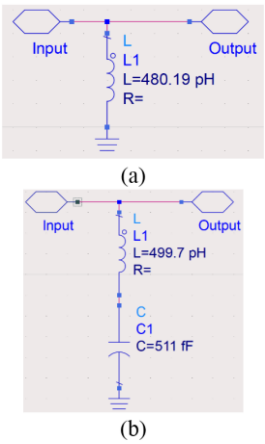

Figure 11: The equivalent circuit design at (a) low frequency range (b) high frequency range

For Design B, there are two stop bands created with the lowest S21 occur at 2.77GHz and 3.3GHz, as shown in Figure 12 (a). At 2.77GHz, $L1$ = 320.88pH and $C1$ = 7.88pF

are used to perform stop band. Meanwhile, another stop band has *L2* and *C2*, which are equal to 644.7pH and 4.96pF respectively. There is only one stop band that occurs at high frequency range in Figure 12 (b). Stop band with the lowest S21 at 10.13GHz is produced by *L1* = 344pH and *C1* = 713.8fF.

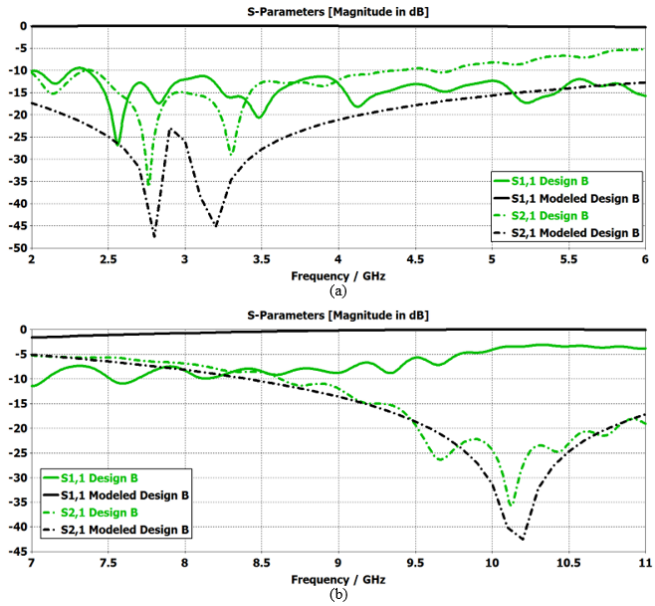

Figure 12: The results of S-parameters from Design B and equivalent circuit design at (a) low frequency range (b) high frequency range

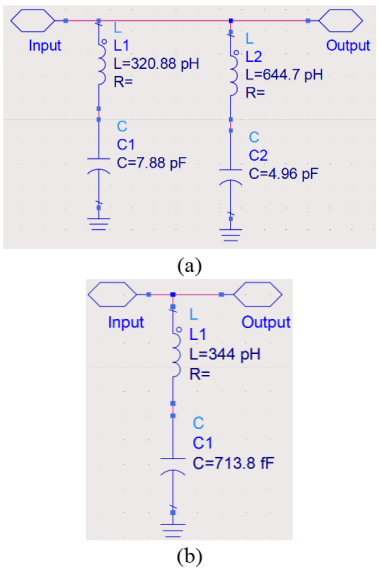

Figure 13: The equivalent filter circuit design at (a) low frequency range (b) high frequency range

At low frequency range, Design C shows almost stop band with the lowest S21 that occurs at 3.21GHz in Figure 14 (a). The stop band is created by *L2* = 13.44pH and *C2* = 157.55pF. Meanwhile, there is also pass band created by *L1* = 11.2pH and *C1* = 33.45pF to pass at 2.1GHz-2.96GHz. Design C demonstrates pass band at high frequency range as shown in Figure 14 (b). The pass band is produced by *L1* and *C1* with 45.71pH and 5.68pF respectively.

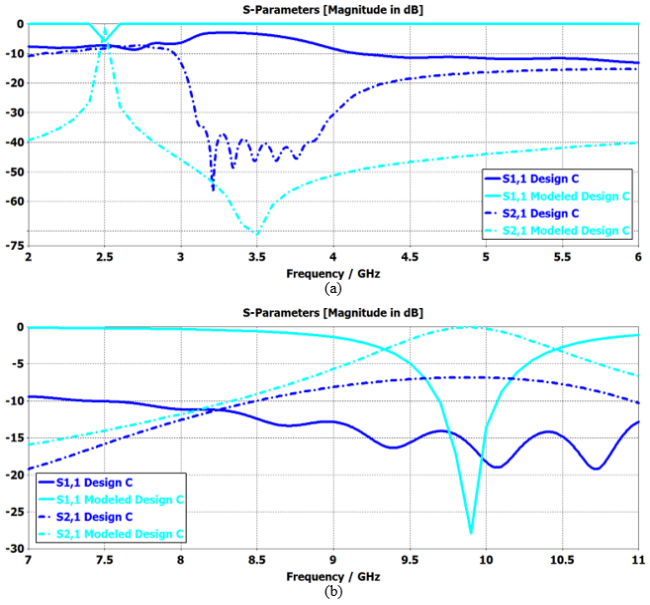

Figure 14: The results of S-parameters from Design C and equivalent circuit design at (a) low frequency range (b) high frequency range

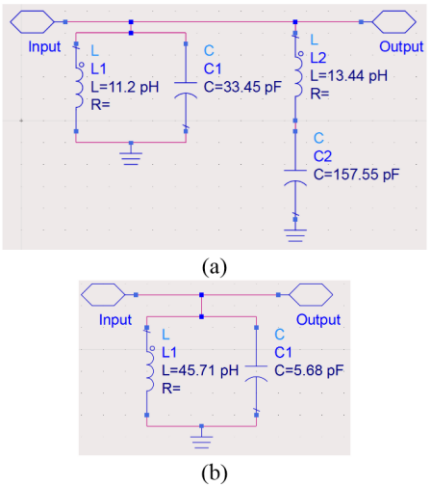

Figure 15: The equivalent filter circuit design at (a) low frequency range (b) high frequency range

Design D performs almost stop band at low frequency range with *L2* = 49.22pH and *C2* = 31.29pF in Figure 17 (a). However, there is a narrow pass band occurs at 2.18GHz-2.42GHz. The pass band is created by *L1* = 79.26pH and *C1* = 17.54pF. At high frequency range, Design D shows pass band at 9.5GHz-11GHz as shown in Figure 16 (b). *C1* of 1.35pF is used to perform the pass band. At high frequency range, stop band with the lowest S21 occurs at 8.04GHz. *L1* = 367.79pH and *C2* = 1.07pF creates the stop band.

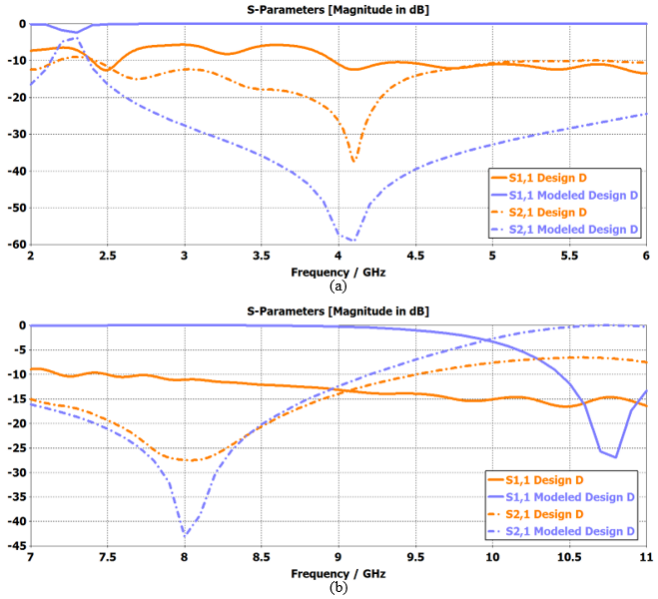

Figure 16: The results of S-parameters from Design D and equivalent circuit design at (a) low frequency range (b) high frequency range

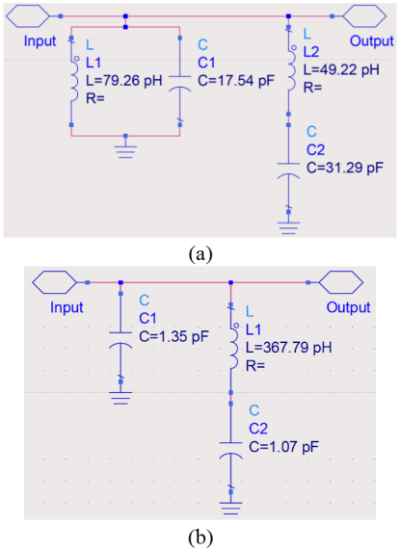

Figure 17: The equivalent circuit design at (a) low frequency range (b) high frequency range

Copper waveguide performs high pass at frequency more than cut off frequency of 2.76GHz. Design A and Design B show closer response to achieve pass band around 4GHz-8GHz. Meanwhile, Design C and Design D achieve pass band around 9GHz-11GHz. This shows that the square DWS with horizontal connecting strips behaves almost the same characteristics as the square DWS with a gap separated in between them. The same characteristics are also performed by the square DWS with vertical connecting strips and the square DWS with both horizontal and vertical connecting strips. This also shows that the design vertical connecting strips have significant effects compared to horizontal connecting strip.

Copper waveguide achieves high pass and thus consists of *L* and *R* for equivalent circuit. Design A achieves high pass, while Design B achieves two stop bands at low frequency range. However, stop band is performed at high frequency range for both Design A and Design B. Different value of *L* and *C* are used due to different lowest S21 value are obtained. Design C and Design D show stop band and pass band at low frequency range. The differences in bandwidth and the lowest S21 cause the differences in value of *L* and *C*. At high frequency range, both Design C and Design D achieve pass band.

IV. Conclusion

In this paper, the waveguide with defected waveguide structure (DWS) is presented. DWS design can show pass band and stop band responses. Design A and Design B have closer characteristics to perform pass band at 4GHz-8GHz with the highest S21 that occur at 6GHz achieves -3.82dB and -5.23dB respectively. The closer characteristics are also performed by Design C and Design D. They show stop band at 3GHz-9GHz with the lowest S21 of -56.26dB and -37.47dB that occur at 3.21GHz and 4.1GHz respectively. Pass band is achieved by them at 9GHz-11GHz. In future, the connecting strips of square DWS is designed in meander line to shorten the gap separation.

Acknowledgment

Authors would like to acknowledge the support from Universiti Teknikal Malaysia Melaka (UTeM) and Ministry of Higher Education (MOHE) during the project work. The financial support by UTeM Zamalah Scheme is also gratefully acknowledged.

References

[1] H. L. Zhu, C. Ding, G. Wei and Y. J. Guo, "A novel base station antenna based on rectangular waveguide," *International Symposium on Antennas and Propagation (ISAP), Okinawa*, pp. 196-197, 2016.

[2] S. W. Wong, R. S. Chen, J. Y. Lin, L. Zhu and Q. X. Chu, "Substrate integrated waveguide quasi-elliptic filter using slot-coupled and microstrip-line cross-coupled structures," *IEEE Transactions on Components, Packaging and Manufacturing Technology*, vol. 6, no. 12, pp. 1881-1888, December 2016.

[3] C. Zhao, C. Fumeaux and C. C. Lim, "Folded substrate-integrated waveguide band-pass post filter," *IEEE Microwave and Wireless Components Letters*, vol. 27, no. 1, pp. 22-24, January 2017.

[4] R. V. Snyder and S. Bastioli, "V-band waveguide bandpass filter with wide stopband and harmonics absorption," *46th European Microwave Conference (EuMC), London*, pp. 245-248, 2016.

[5] K. Uyama, S. Nishimura, H. Deguchi and M. Tsuji, "Transmission characteristics of CRLH rectangular waveguides constructed by the cutoff modes of TM and TE waves," *International Conference on Electromagnetics in Advanced Applications (ICEAA), Cairns, QLD*, pp. 728-731, 2016.

[6] S. Gite and D. Niture, "A compact printed monopole antenna for TV white space applictions using defected ground structure," *International Conference on Information Processing (ICIP), Pune*, pp. 198-200, 2015.

[7] G. S. Kunturkar and P. L. Zade, "Design of fork-shaped multiband monopole antenna using defected ground structure," *International Conference on Communications and Signal Processing (ICCSP), Melmaruvathur*, pp. 0281-0285, 2015.

[8] F. Raval, Y. P. Kosta, J. Makwana and A. V. Patel, "Design & implementation of reduced size microstrip patch antenna with metamaterial defected ground plane," *International Conference on Communication and Signal Processing, Melmaruvathur*, pp. 186-190, 2013.

[9] J. Vijayakrishnan and R. P. Dwivedi, "Analysis of different shapes of defected microstrip structure (DMS) and their stop-band performance," *ARPN Journal of Engineering and Applied Sciences*, vol. 10, no. 8, May 2015.

[10] M. A. Samad and A. K. Hamid, "Miniaturization of waveguide antenna using square/circular arrays of SRR," *5th International Conference on Electronic Devices, Systems and Applications (ICEDSA), Ras Al Khaimah*, pp. 1-4, 2016.

[11] D. M. Pozar, *Microwave engineering*, 4th edition. New Jersey: John Wiley & Sons, INC, 2012, pp. 408-415.